SECURITY CLASSIFICATION OF THIS PAGE

DTIC ELECTE AUG 16 1993 S A D

AD-A267 908

REPORT DOCUMENTATION

Approved No. 0704-0188

1a. REPORT SECURITY CLASSIFICATION

2a. SECURITY CLASSIFICATION AUTHORITY

2b. DECLASSIFICATION / DOWNGRADING SCHEDULE

3. DISTRIBUTION / AVAILABILITY OF REPORT

unlimited

4. PERFORMING ORGANIZATION REPORT NUMBER(S)

AFOSR - F49620 - 92 - J - 0400

5. MONITORING ORGANIZATION REPORT NUMBER(S)

AFOSR-TR- 93 0594

6a. NAME OF PERFORMING ORGANIZATION

California Institute of Technology

6b. OFFICE SYMBOL (If applicable)

7a. NAME OF MONITORING ORGANIZATION

Same as 8a

6c. ADDRESS (City, State, and ZIP Code)

Department of Electrical Engineering
MS 116-81
Pasadena CA 91125

7b. ADDRESS (City, State, and ZIP Code)

Same as 8c

8a. NAME OF FUNDING / SPONSORING ORGANIZATION

AFOSR

8b. OFFICE SYMBOL (If applicable)

NE

9. PROCUREMENT INSTRUMENT IDENTIFICATION NUMBER

F49620-92-J-0400

8c. ADDRESS (City, State, and ZIP Code)

110 Duncan Ave Suite B115
BAFB DC 20332-0001

10. SOURCE OF FUNDING NUMBERS

PROGRAM ELEMENT NO.	PROJECT NO.	TASK NO.	WORK UNIT ACCESSION NO.
61102F	2305	DS	

11. TITLE (Include Security Classification)

3-D Optical Memory Disk

12. PERSONAL AUTHOR(S)

Demetri Psaltis

13a. TYPE OF REPORT	13b. TIME COVERED	14. DATE OF REPORT (Year, Month, Day)	15. PAGE COUNT
Annual Technical	FROM 7/1/92 TO 6/30/93	7/23/93	21

16. SUPPLEMENTARY NOTATION

17. COSATI CODES			18. SUBJECT TERMS (Continue on reverse if necessary and identify by block number)
FIELD	GROUP	SUB-GROUP	

19. ABSTRACT (Continue on reverse if necessary and identify by block number)

In this report we describe optical disks that store data holographically in three dimensions using either angle multiplexing or wavelength multiplexing. Data is stored and retrieved in parallel blocks or pages, each page consisting of approximately one million bits. The storage capacity of such disks is derived as a function of disk thickness, pixel size, page size and scanning parameters. The optimum storage density is approximately 120 bits/μm^2.

93-18778

20. DISTRIBUTION / AVAILABILITY OF ABSTRACT

☑ UNCLASSIFIED/UNLIMITED ☐ SAME AS RPT. ☐ DTIC USERS

21. ABSTRACT SECURITY CLASSIFICATION

Unclass

22a. NAME OF RESPONSIBLE INDIVIDUAL

Craig

22b. TELEPHONE (Include Area Code)

202-767-4931

22c. OFFICE SYMBOL

NE

DD Form 1473, JUN 86 Previous editions are obsolete. SECURITY CLASSIFICATION OF THIS PAGE

Grant AFOSR-F49620-92-J-0400

Annual Technical Report

3-D OPTICAL MEMORY DISK

Demetri Psaltis

Submitted to:

Dr. Alan E. Craig

Air Force Office of Scientific Research

Bolling Air Force Base, Washington, DC.

Accesion For		
NTIS	CRA&I	☑
DTIC	TAB	☐
Unannounced		☐
Justification		
By		
Distribution /		
Availability Codes		
Dist	Avail and / or Special	
A-1		

Principal Investigator:

Dr. Demetri Psaltis

California Institute of Technology

Department of Electrical Engineering

Pasadena, California 91125

ABSTRACT

In this report we describe optical disks that store data holographically in three dimensions using either angle multiplexing or wavelength multiplexing. Data is stored and retrieved in parallel blocks or pages, each page consisting of approximately one million bits. The storage capacity of such disks is derived as a function of disk thickness, pixel size, page size, and scanning parameters. The optimum storage density is approximately 120 bits/μm^2.

1. Introduction

Holographic storage of data in 3-D media such as photorefractive crystals can provide high storage density and fast parallel access to the stored information. Such memories were investigated very extensively in the early 60's [1–5]. Even though these early efforts produced remarkable results they never found practical application largely because of material limitations such as low sensitivity, fanning, and hologram decay. Interest in holographic 3-D memories has been revitalized in recent years for a variety of reasons, including significant advances in recording materials (photorefractive and photopolymers), dramatic improvements in all optical devices (lasers, spatial light modulators, detectors, etc.), and most significantly, the emergence of applications, such as neural networks, machine vision, and databases, that can make use of the capabilities of holographic 3-D memories. The theoretical upper limit on the storage density is V/λ^3, where V is the volume of the hologram and λ is the wavelength of the light. This limit is in the order of 10^{12} bits per cm^3, however in practical systems only 10^9–10^{10} bits per cm^3 is achievable due to the finite numerical aperture of the optical system that transfers the data into the optical system and the dynamic range of the crystal. For example, 10^3 can be superimposed at the same location, each hologram consisting of $10^3 \times 10^3$ pixels, giving a total memory of 10^9 bits per location. The practical usefulness of such a memory must be considered in light of the fact that electronic RAM memory chips currently under development have storage density of 64 million bits [6]. Twenty such chips mounted on a single board could match the storage capability of the volume hologram. In order to build a mass storage medium that is not threatened by semiconductor memories, we must construct holographic memories that have a capacity much larger than 10^9 bits.

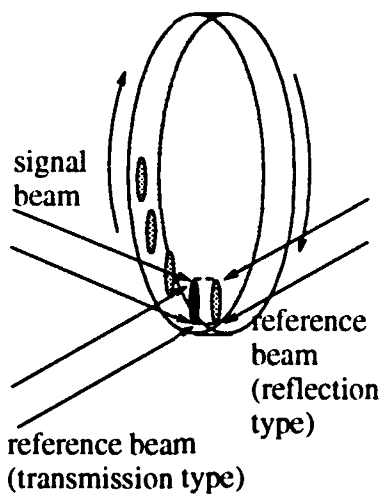

Figure 1. The 3-D holographic disk (HD).

In this report, we present a spatially multiplexed 3-D holographic storage scheme that we refer to as the 3-D holographic disk (HD) [7]. As in all spatial multiplexing schemes, the most crucial component of the

system is the scanning mechanism that steers the readout mechanism to different locations on the disk. In our system, spatial multiplexing is done in a disk configuration with the rotation used to access different recording locations, as shown in Figure 1. Two light beams (a signal and a reference) interfere inside the photorefractive crystal to create a phase grating via the photorefractive effect. Multiple holograms are recorded at the same location by changing the reference beam angle (angle multiplexing) or by changing the wavelengths of the reference and signal beams (wavelength multiplexing). Because of the Bragg-matching requirement of volume holograms, individual holograms can be read out by changing the direction of the reference beam (for angle multiplexing), or the wavelength of the reference beam (for wavelength multiplexing). We will assume throughout that the image beam is at normal incidence on the crystal.

The main result of this report is the derivation of the storage capacity of 3-D HDs as limited by geometrical constraints. We show that a 3-D disk of approximately 1.5 cm thick has storage density approximately equal to 120 bits/μm^2. Thus, a 3-D HD stores the equivalent of more than a hundred conventional 2-D disks of the same area.

2. Angle Multiplexed Holographic Disk

In this section we address the following question: What is the maximum number of bits, N, that can be stored in a 3-D HD of area A using angle multiplexing? We will show that in order to maximize N we must properly select the thickness of the HD (L), the magnification of the optical system that transfers the data to the disk, and the angles of incidence for the reference beam. In what follows we derive these optimum parameters. The limits to storage capacity in this report are due to geometrical constraints. The dynamic range of the recording material imposes a limit on storage density independently. We will see that the capacity due to the geometric constraints is more restrictive than the material limitations in the 3-D HD system.

We can express N as follows:

$$N = N_s N_\theta N_p^2 \, . \tag{1}$$

In the above equation N_s is the number of separate locations on the disk where holograms are superimposed, N_θ is the number of holograms that are angularly multiplexed at the same location, and N_p^2 is the number of pixels in each stored hologram. We will derive an expression for each of the three quantities and then maximize their product with respect to the various parameters of the system.

2a. Maximum Number of Angularly Multiplexed Holograms

We derive an expression for the maximum number of holograms, N_θ, that can be angularly multiplexed at a single location. In the following analysis data is stored by recording either reflection or transmission

holograms. The reference beam is a planewave whose incident angle is θ_R. The signal beam can be considered as a superposition of planewaves that spans a range of angles. To calculate N_θ we must first calculate $\Delta\theta_R$, the full width of the angular selectivity of each hologram, which we take to be the angular separation between adjacent holograms. An approximate expression for $\Delta\theta_R$ is [8]

$$\Delta\theta_R = \frac{8\lambda}{n\pi L}\frac{\cos\theta_S}{|\sin(\theta_R+\theta_S)|}. \tag{2}$$

where λ is the wavelength, L is the thickness of the hologram, n is the index, and θ_S is the incident angle of the central planewave component of the signal beam (see Figure 2). For transmission holograms $0 < |\theta_R| < \pi/2$, and for reflection holograms $\pi/2 < |\theta_R| < \pi$. The signal beam is assumed to be in the range $0 < |\theta_S| < \pi/2$.

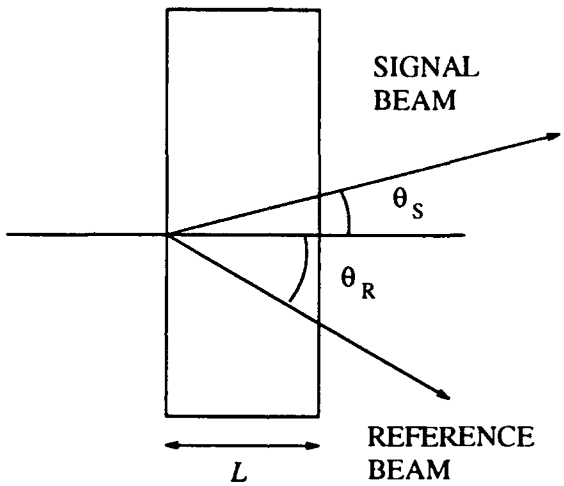

Figure 2. Recording geometry.

Eq. (2) is only an approximate estimate for the angular selectivity of the entire grating since different planewave components have different $\Delta\theta_R$. However, Eq. (2) is commonly used for setting the angular separation between reference beam angles. The cross-talk resulting when holograms are angularly multiplexed in this way has been calculated recently [9].

To calculate the number of holograms that can fit into a range of reference beam angles θ_R spanning from θ_1 to θ_2 (each hologram being separating from its adjacent holograms by a corresponding $\Delta\theta_R$), we observe that

$$|\sin(\theta_R+\theta_S)|\Delta\theta_R = \frac{8\lambda}{n\pi L}\cos\theta_S, \tag{3}$$

which is valid for all possible angles θ_R. If we add together $N_\theta - 1$ such equations, one for each value of θ_R, and approximate the left hand side of the summation by an integral, we obtain the following expression:

$$\int_{\theta_1}^{\theta_2} |\sin(\theta_R + \theta_S)| d\theta_R = \frac{8\lambda(N_\theta - 1)}{n\pi L} \cos\theta_S. \tag{4}$$

Solving for the number of reference angles, we get

$$N_\theta = 1 + \left(\frac{n\pi L}{8\lambda}\right) \frac{|\cos(\theta_S + \theta_1) - \cos(\theta_S + \theta_2)|}{\cos\theta_S}, \tag{5}$$

where it is assumed that either $0 < \theta_S + \theta_1 < \theta_S + \theta_2 < \pi$, or $-\pi/2 < \theta_S + \theta_1 < \theta_S + \theta_2 < 0$. Physically, this means that the reference beam is always to one side of the signal beam. The above calculations were carried out for angles inside the crystal. We can use Snell's law to convert to angles outside the crystal.

In the following, we will assume that the image beam has normal incidence ($\theta_S = 0$). In this case, Eq. (5) becomes

$$N_\theta = 1 + \left(\frac{n\pi L}{8\lambda}\right) |\cos\theta_1 - \cos\theta_2|, \tag{6}$$

where we have $0 < \theta_1 < \theta_2 < \pi/2$ for transmission holograms. We can increase N_θ by a factor of 2 by recording a second set of angularly multiplexed holograms in the range $-\theta_1$ to $-\theta_2$, since the number of holograms that can be angularly multiplexed in the same range of angles is equal to the expression in Eq. (6). It is also possible to simultaneously angularly multiplex reflection and transmission holograms, as shown in Figure 3. Therefore, the geometric limit on the total number of holograms that can be superimposed in the same location is 4 times the expression in Eq. (6) .

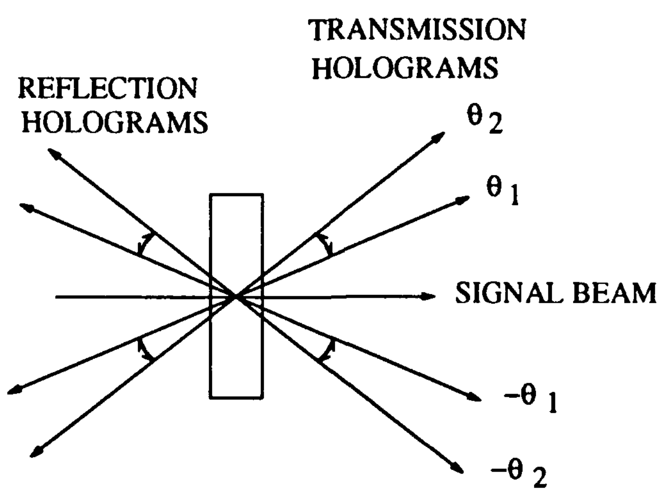

Figure 3. Angular multiplexing by reflection and transmission holograms from both sides of the signal beam.

2b. Spatial Multiplexing

The number of non-overlapping spatial locations on a disk with area A is

$$N_s = \frac{A}{a} = \frac{A}{ww'}, \tag{7}$$

where $a = w \times w'$ is the area of each location. To determine w and w' we need to take into account the fact that the stored images can be in exact focus at only one plane in the volume of the crystal. As the thickness of the crystal increases, the area occupied by the defocused image at the surface of the hologram also increases. Moreover, the size of the area that is illuminated by the off-axis reference beam increases in one dimension as the crystal thickness and the angular sweep increase. We will derive expressions for w and w' with reference to the geometry of Figure 4. We assume that the images to be stored are at normal incidence and are focused at the middle of the crystal. We can calculate the extent of the defocused image on the surfaces by tracing the rays corresponding to the highest spatial frequency of the focused image. Let δ be the resolution or pixel spacing of the focused image. Then the maximum spatial frequency is approximately $1/\delta$, corresponding to a diffracted plane wave traveling at an angle $\theta = \sin^{-1}(\lambda/n\delta)$. We use the ray optics approximation to trace this maximum spatial frequency component and obtain the size of the defocused image at the crystal faces:

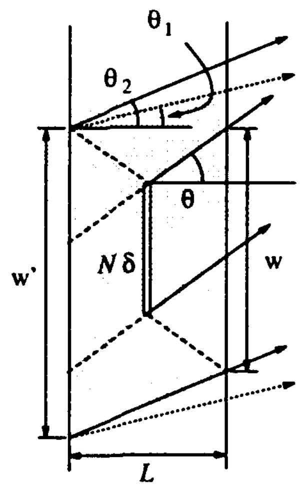

Figure 4. Angle multiplexing: extra area taken up by defocusing and reference beam angle change.

$$w = N_p\delta + L\tan\theta = N_p\delta + \frac{L}{\sqrt{(n\delta/\lambda)^2 - 1}}. \tag{8}$$

As shown in Figure 4, in order for the reference beam to fully illuminate the volume of the crystal that the signal beam occupies, it must illuminate a width larger than w in the direction of reference beam sweep. From the geometry of Figure 4, this width is

$$w' = w + L\tan\theta_2. \tag{9}$$

The overall area that must be devoted to each recording location is therefore

$$a = ww' = w(w + L\tan\theta_2), \tag{10}$$

where w is given by Eq. (8).

2c. Optimum N_p, θ_1, and δ

We can now write an expression for N, the total number of bits stored, by using Eqs. (7)-(10) and Eq. (1):

$$N = AN_p^2\,\frac{N_\theta}{ww'} = AN_p^2\,\frac{1 + \frac{n\pi L}{4\lambda}(\cos\theta_1 - \cos\theta_2)}{\left[N_p\delta + \frac{L}{\sqrt{(n\delta/\lambda)^2-1}}\right]\left[N_p\delta + \frac{L}{\sqrt{(n\delta/\lambda)^2-1}} + L\tan\theta_2\right]}. \tag{11}$$

We wish to maximize the above expression by optimally selecting N_p, L, θ_1, θ_2, and δ, which are the parameters we can control.

First of all, we note that N decreases monotonically as θ_1 increases (in our analysis $0 < \theta_1 < \pi/2$), therefore $\theta_1 = 0$ is the optimum value. However, since the angular selectivity is very poor around $\theta_1 = 0$, in practice the minimum angle of the reference is set at $\theta_1 \approx 10°$ inside the crystal. Next we consider the optimum number of pixels, N_p. Taking the derivative of N with respect to N_p shows that N is a monotonically increasing function of N_p. This result confirms our intuition since the increase in the disk area required to store the holograms due to defocusing and angular multiplexing can be thought of as an "edge" effect. The use of larger images implies fewer recording locations on the same disk area, and hence fewer edges. In practice N_p is limited by the number of pixels of the spatial light modulator (SLM) to approximately $N_p = 1,000$. For the rest of this section, we will consider θ_1 and N_p as given and fixed.

The determination for the three remaining variables (L, θ_2, and δ) is more difficult. We first consider the optimum pixel size δ. For a given L, N is maximized with respect to δ when w is minimized with respect to δ. To find the optimum δ it is convenient to write w as

$$w = \frac{\lambda N_p}{n}\left(y^{3/2} + \frac{c^{3/2}}{\sqrt{y^3 - 1}}\right), \tag{12}$$

where

$$y = \left(\frac{n\delta}{\lambda}\right)^{2/3} \tag{13}$$

and

$$c = \left(\frac{nL}{\lambda N_p}\right)^{2/3}. \tag{14}$$

To minimize w with respect to δ, we diffe entiate w with respect to y (since y increases monotonically with δ) and set the derivative to zero. This yields the following equation for y

$$y^3 = cy + 1. \tag{15a}$$

The solution to this cubic equation is

$$y = \sqrt[3]{\frac{1}{2} + \sqrt{\frac{1}{4} - \frac{c^3}{27}}} + \sqrt[3]{\frac{1}{2} - \sqrt{\frac{1}{4} - \frac{c^3}{27}}} \tag{15b}$$

which can be evaluated for a given L to yield the optimum δ. Once y is determined we can solve for the optimum pixel spacing, δ_o, from the following equation:

$$\delta_o = \frac{\lambda}{n}\, y^{3/2}. \tag{16}$$

It can be shown that δ_o increases as L increases.

The above solution, however, may not always be realizable. In any practical system, the minimum δ (denoted as δ_{min}) is limited by the imaging system to a value larger than the wavelength λ. If we use an imaging lens of F/number z, the smallest resolvable spot is

$$\delta_{min} = \lambda\sqrt{4z^2 + 1}, \tag{17}$$

which corresponds to the highest spatial frequency planewave traveling at an angle

$$\theta_i = \sin^{-1}\left(\frac{\lambda}{\delta}\right). \tag{18}$$

Inside the crystal, this becomes (from Snell's law)

$$\begin{aligned}\theta_r &= \sin^{-1}\left(\frac{1}{n}\sin\theta_i\right)\\ &= \sin^{-1}\left(\frac{\lambda}{n\delta_{min}}\right).\end{aligned} \tag{19}$$

Therefore the smallest resolvable spot size inside the crystal is also δ_{min} as given by Eq. (17).

δ_{min} is the lower bound for the size of δ. If L is too small, δ_o (from Eq. (15)) becomes less then δ_{min}. In that case, we set $\delta = \delta_{min}$. Since δ_o increases as L increases, we can use Eqs. (13)–(16) to find the smallest L for which δ_o is larger than δ_{min}:

$$L_{min} = \frac{\lambda N_p}{n}\left(\frac{y_{min}^3 - 1}{y_{min}}\right)^{2/3}, \tag{20}$$

where

$$y_{min} = \left(\frac{n\delta_{min}}{\lambda}\right)^{2/3}. \tag{21}$$

We will refer to the condition where the optimum δ is less than δ_{min} as the "thin" disk regime. If, on the other hand, the optimum pixel spacing is larger than the resolution limit of the lens, this corresponds to the "thick" regime. For example, for $n = 2.2$, $\lambda = 500$ nm, $N_p = 1000$, and using a F/3 imaging lens (i.e., $z = 3$), we get $\delta_{min} = 3.04\ \mu$m and $L_{min} = 40.36$ mm. Note that L_{min} does not depend on θ_2.

To summarize, if $L > L_{min}$ (thick disk), we use $\delta = \delta_o$ (from Eq. (15)), and if $L < L_{min}$ (thin disk), we use $\delta = \delta_{min}$ (as given by Eq. (17)).

2d. Optimum Thickness L

Our problem is now reduced to maximizing N with respect to the two remaining variables L and θ_2. We first treat θ_2 as fixed, and find the optimum L that maximizes N/A.

In the range $L < L_{min}$ we use δ_{min} as the optimum δ, and write N/A from Eq. (11) as

$$N/A = \frac{1}{\delta_{min}^2} \frac{1 + \alpha x}{(1 + \beta x)(1 + \gamma x)} \tag{22}$$

where

$$x = \frac{nL}{\lambda N_p}, \tag{23}$$

$$\alpha = \frac{\pi N_p}{8} (\cos\theta_1 - \cos\theta_2), \tag{24}$$

$$\beta = \frac{1}{y_{min}^{3/2} \sqrt{y_{min}^3 - 1}}, \tag{25}$$

and

$$\gamma = \beta + \frac{\tan\theta_2}{y_{min}^3}. \tag{26}$$

We can solve for the optimum L by differentiating the expression in Eq. (22) with respect to x. The maximum N/A turns out to be

$$N/A = \frac{1}{\delta_{min}^2} \frac{\alpha/\beta\gamma}{\left(\sqrt{\frac{1}{\beta} - \frac{1}{\alpha}} - \sqrt{\frac{1}{\gamma} - \frac{1}{\alpha}}\right)^2}, \tag{27}$$

which occurs at

$$L = L_o = \frac{\lambda N_p}{n} \left(-\frac{1}{\alpha} + \sqrt{\left(\frac{1}{\beta} - \frac{1}{\alpha}\right)\left(\frac{1}{\gamma} - \frac{1}{\alpha}\right)} \right), \tag{28}$$

assuming of course that $L_o < L_{min}$. If $L_o > L_{min}$ this means that the optimum thickness is out of the thin regime where the analysis used to derive L_o applies. Within the thin regime the maximum thickness L occurs at the boundary since N/A is monotonically increasing with L for $L < L_{min}$. To obtain the overall optimum thickness L we must compare the maximum obtained from this regime (i.e., $L \le L_{min}$) with the

optimum thickness obtained from the thick regime ($L > L_{min}$) and finally select the thickness that yields the larger density N/A.

As an example, we continue with the previous example where $\delta_{min} = 3.04\ \mu m$ (for a lens with F/number of 3). If we take $\theta_1 = 10°$ and $\theta_2 = 20°$, we find L_o to be 16.74 mm, which is less than $L_{min} = 40.36$ mm. Therefore, the solution obtained from the thin regime is the valid optimum thickness. Note that as N_p increases, so does α, and therefore the expression in Eq. (27) increases. For large N_p, the maximum N/A as given by Eq. (27) increases approximately linearly with N_p, or the square root of the total number of pixels N_p^2.

For $L > L_{min}$, we can use Eq. (16) for δ and using Eqs. (12)–(15), Eq. (11) can be written as

$$N/A = \left(\frac{n}{\lambda}\right)^2 \frac{1 + \alpha c^{3/2}}{\left(y^{3/2} + \frac{c^{3/2}}{\sqrt{y^3 - 1}}\right)\left(y^{3/2} + \frac{c^{3/2}}{\sqrt{y^3 - 1}} + c^{3/2}\tan\theta_2\right)}. \tag{29}$$

The above expression can be evaluated numerically to find the value of L which maximizes N/A. We can also derive a relatively simple asymptotic expression (for large L) by observing that as $L \to \infty$, $y \to \sqrt{c}$. The asymptotic expression for N/A is

$$N/A \to \left(\frac{n}{\lambda}\right)^2 \frac{\pi N_p(\cos\theta_1 - \cos\theta_2)}{16\tan\theta_2}\sqrt{\frac{\lambda N_p}{nL}}. \tag{30}$$

The above expression predicts that the density will decrease as the disk thickness becomes very large. This is confirmed by the numerical results we present in the following section.

2e. Optimum θ_2 and the Maximum Storage Density

The final step in the optimization of the storage density N/A, consists of optimally selecting θ_2. Since we cannot analytically derive the optimum angle, we resort to numerical methods. In Figure 5 we plot Eq. (22) in the thin regime (solid line) and Eq. (29) in the thick regime (dotted line) as a function of L for various values of θ_2 using the optimum value for δ. The vertical line indicates the transition from one regime to the other. The optimum values for L and θ are those that yield the maximum density. The parameters used in plotting Fig. 5 are $\lambda = 500$ nm, $N_p = 1,000$, $n = 2.2$ (the index of refraction for $LiNbO_3$ crystals), and $\theta_1 = 10°$. $\theta_2 = 30°$ is the maximum value for which N/A is plotted since 27.04° is the largest angle that can be supported inside the crystal (due to Snell's law) without resorting to the use of index matching fluids.

From Figure 5, we see that the maximum N/A is obtained near $L = 1.5$ cm and increases monotonically with θ_2 for the parameters we selected. In this case, the optimum thickness is in the thin regime ($L_o < L_{min}$). Since it is not practical to use $\theta_2 = 30°$ inside the crystal (the critical angle is 27.04°), we get a realistic estimate for the achievable density by using $\theta_2 = 20°$. The corresponding angle swing outside the crystal is then 22.5° to 48.8° (total angular swing of 26.3°) which is practically achievable. The maximum density

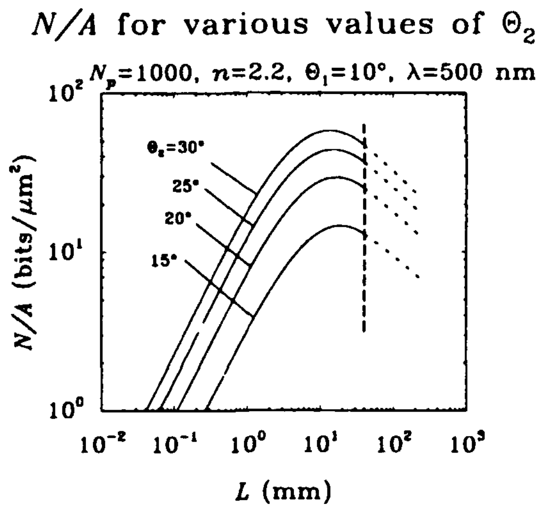

Figure 5. Angle multiplexing: N/A vs. L for various values of θ_2. We take $N_p = 1000$, $n = 2.2$, $\lambda = 500$ nm, and $\theta_1 = 10°$.

N/A is 29.3 bits/μm^2, which is obtained for a crystal thickness of $L = 16.74$ mm using $N_\theta = 1306$ angularly multiplexed holograms. This density can be increased by a factor of 4 (giving us $N/A = 117.2$ bits/μm^2) if we simultaneously record reflection and transmission holograms in the same reference angle range from both sides of the signal beam, as shown in Figure 3. The area for each recording location is $w \times w' = 4.3 \times 10.4\ mm^2$. Figure 6 is a plot of the optimum density and also the number of angularly multiplexed holograms, N_θ, as a function of L. For the thickness that yields maximum density, $N_\theta = 1,306$ holograms. Since more than 5,000 holograms have been recorded and faithfully reproduced in Lithium Niobate [10], the geometric factors considered in this report limit the recording more severely than the material dynamic range. As another example, if we record only 100 holograms at each location, then the optimum thickness is a little over 1 mm and the corresponding storage density is about 8.8 bits/μm^2 (compared to about 30 bits/μm^2 for the optimum design). This density can be increased by a factor of 4 as we already described in Figure 3.

3. Wavelength Multiplexing

Wavelength multiplexing [11–12] is an alternative method for multiplexing holograms in a single location on the HD. In this section we calculate the capacity of a wavelength multiplexed HD using a similar derivation as for angular multiplexing. The number of bits that can be stored is expressed as

$$N = N_s N_\lambda N_p^2, \tag{31}$$

where N_λ is the number of wavelength multiplexed holograms. We assume that the wavelength λ sweeps from λ_1 to λ_2, with $\lambda_1 < \lambda_2$.

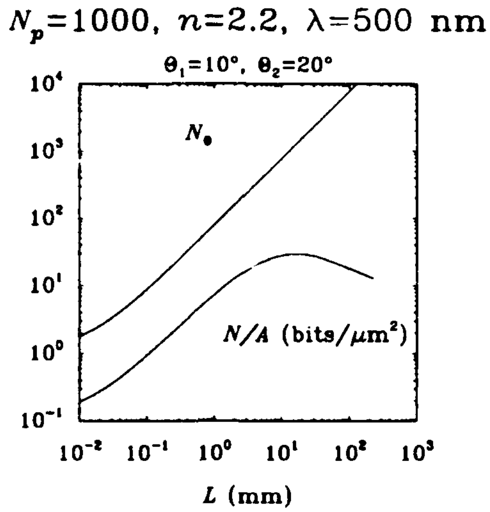

Figure 6. Angle multiplexing: optimum N/A (optimized with respect to δ) and N_p as functions of thickness L. We take $N_p = 1000$, $n = 2.2$, $\lambda = 500$ nm, $\theta_1 = 10°$, and $\theta_2 = 20°$.

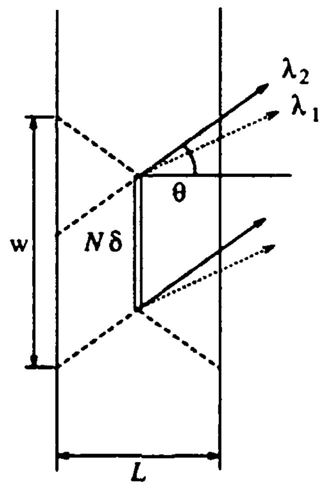

Figure 7. Wavelength multiplexing: extra area taken up because of defocusing and wavelength change.

For wavelength multiplexing, we again assume that the image is at normal incidence and focused at the middle of the crystal (Figure 7), and that the reference beam is counter-propagating with the image beam also at normal incidence. In this case, the problem of image defocusing at the crystal surface is the same, and we get Eq. (8) for the width w as before. However, since the reference beam is co-linear with the signal beam for all wavelengths, there is no extra width taken up by the $L\tan\theta_2$ term in the expression for w' in Eq. (9). On the other hand, as λ sweeps through λ_1 to λ_2, w changes. For any choice of δ, the largest w is for $\lambda = \lambda_2$. Therefore we have

$$N_s = \frac{A}{w^2}, \tag{32}$$

where

$$w = N_p\delta + \frac{L}{\sqrt{(n\delta/\lambda_2)^2 - 1}} \tag{33}$$

is a function of λ_2.

To find N_λ, we note that the half-width of the (frequency) selectivity $\Delta\nu$ is [8]

$$\Delta\nu = \frac{v_c}{nL}, \tag{34}$$

where v_c is the speed of light in vacuum. As λ sweeps over λ_1 to λ_2, the number of wavelength multiplexed holograms that can be stored is therefore

$$N_\lambda = 1 + \frac{\nu_1 - \nu_2}{2\Delta\nu} = 1 + \frac{nL}{2}\left(\frac{1}{\lambda_1} - \frac{1}{\lambda_2}\right), \tag{35}$$

where we take the separation between adjacent holograms to be a full width $2\Delta\nu$. Using Eqs. (32), (33), and (35), we then have

$$N = AN_p^2 \frac{1 + \frac{nL}{2}\left(\frac{1}{\lambda_1} - \frac{1}{\lambda_2}\right)}{\left[N_p\delta + \frac{L}{\sqrt{(n\delta/\lambda_2)^2 - 1}}\right]^2}. \tag{36}$$

3a. Optimum N_p, λ_1, and δ

We now want to maximize N with respect to N_p, L, λ_1, λ_2, and δ. As before, N increases monotonically with N_p, which is limited by the SLM to about 1,000. N also increases as the minimum wavelength λ_1 decreases. This will be limited by the shortest usable wavelength we can get out of a tunable laser and/or the spectral sensitivity of the material. For the remainder of this section, we will assume that N_p and λ_1 are given and fixed.

The three remaining parameters λ_2, L, and δ are more complicated. We first take L and λ_2 as fixed, and find the optimum δ. Considering N/A as a function δ, we find as before that the maximum N/A is obtained when w is minimized with respect to δ. We then get the same set of equations as Eqs. (13)–(16), except with λ replaced by λ_2. We also have the same δ_{min} and L_{min} (with λ replaced by λ_2) conditions as given respectively by Eqs. (17) and (20). Note that both δ_{min} and L_{min} scale linearly with wavelength (since y_{min} depends only on n and z, the F/number of the imaging lens). It should be emphasized, that δ_{min} is the resolution of the imaging system using wavelength λ_2. The resolution of the system using λ_1 (which is less than λ_2) is of course better.

In summary, if $L > L_{min}$, we use $\delta = \delta_o$ (from Eq. (15)), otherwise we use $\delta = \delta_{min}$ (as defined in Eq. (17)); in these equations, λ is replaced by λ_2. As an example, for λ_2 = 540 nm and a imaging lens

with F/number of 3, we have $\delta_{min} = 3.28\ \mu$m and $L_{min} = 43.59$ mm. For $\lambda_2 = 750$ nm, these become $\delta_{min} = 4.56\ \mu$m and $L_{min} = 60.54$ mm.

3b. Optimum L and λ_2

We now find the optimum thickness L that maximizes N/A. In the thin regime ($L < L_{min}$) we take $\delta = \delta_{min}$, and write N/A as

$$N/A = \frac{1}{\delta_{min}^2} \frac{1 + \alpha x}{(1 + \beta x)^2}, \tag{37}$$

where

$$x = \frac{nL}{\lambda_2 N_p}, \tag{38}$$

$$\alpha = \frac{N_p}{2} \left(\frac{\lambda_2}{\lambda_1} - 1 \right), \tag{39}$$

and

$$\beta = \frac{1}{y_{min}^{3/2} \sqrt{y_{min}^3 - 1}} \tag{40}$$

By differentiating the expression in Eq. (37) with respect to x, we find the maximum N/A to be

$$N/A = \frac{1}{\delta_{min}^2} \frac{\alpha^2}{4\beta(\alpha - \beta)}, \tag{41}$$

which occurs at

$$L = L_o = \frac{\lambda_2 N_p}{n} \left(-\frac{2}{\alpha} + \frac{1}{\beta} \right). \tag{42}$$

For example, for $\lambda_1 = 500$ nm, $\lambda_2 = 540$ nm ($\lambda_2/\lambda_1 = 1.08$), $n = 2.2$, and $N_p = 1000$, we get $L_o = 43.82$ mm. If λ_2 increases to 750 nm, L_o increase to 60.88 mm. In both cases, L_o is larger than L_{min} (43.59 mm and 60.54 mm respectively). This means that in there is no maximum in the thin regime and therefore in the range $L < L_{min}$, N/A is monotonically increasing with L. In this case, we would select the boundary value (L_{min}) for the best thickness obtainable from the thin regime. Notice that for wavelength multiplexed storage the optimum thickness of the disk can become quite large. Even though we are not considering materials issues in this report, we should point out that the useful thickness of the material in practice can be limited by absorption. In some materials (e.g., Lithium Niobate) it is possible to reduce the absorption by properly preparing the material (e.g., by adjusting the dopant and reduction/oxidation level). The reduced absorption will typically reduce the recording speed of the material for a given light intensity. Therefore, when materials considerations are included in the design process, this trade-off between speed and density will emerge.

In the thick regime, $L > L_{min}$, we use Eqs. (15) and (16) (with λ replaced by λ_2) to obtain δ, and write N/A as

$$N/A = \left(\frac{n}{\lambda_2}\right)^2 \frac{1+\alpha c^{3/2}}{\left(y^{3/2} + \frac{c^{3/2}}{\sqrt{y^3-1}}\right)^2}, \tag{43}$$

where α is given by Eq. (39). As before, as $L \to \infty$, $y \to \sqrt{c}$. For wavelength multiplexing, however, the asymptotic behavior of N/A is different. As $L \to \infty$, N/A saturates and approaches

$$N/A \to \frac{n^2 N_p}{8} \frac{1}{\lambda_2} \left(\frac{1}{\lambda_1} - \frac{1}{\lambda_2}\right). \tag{44}$$

Thus for the range $L > L_{min}$, N/A also increases monotonically with L.

Note that the saturation value of N/A increases as N_p increases and λ_1 decreases. Also, for any choice of λ_2/λ_1, we have

$$\frac{1}{\lambda_2}\left(\frac{1}{\lambda_1} - \frac{1}{\lambda_2}\right) \leq \frac{1}{4\lambda_1^2}, \tag{45}$$

with equality at

$$\frac{\lambda_2}{\lambda_1} = 2. \tag{46}$$

Thus, even if it is practical to have a light source with such a large range of wavelength tunability, the optimum setting for λ_2/λ_1 in order to obtain maximum saturation density is 2 (provided we use the same λ_1). For practical systems, λ_2/λ_1 is smaller than 2, and in this range the saturation value of N/A increases as λ_2/λ_1 increases. In the case where $\Delta\lambda = \lambda_2 - \lambda_1 \ll \lambda_1$ ($\lambda_2 \approx \lambda_1$), the saturation value given in Eq. (44) is approximately

$$N/A \approx \frac{n^2 N_p}{8} \frac{\Delta\lambda}{\lambda_1^3}, \tag{47}$$

which is proportional to $\Delta\lambda$.

In practice, the range of usable wavelengths is determined by the laser system. For instance, dye lasers can be tuned in the range from 370 nm to 890 nm, which gives us a λ_2/λ_1 of 2.40, in excess of the optimum $\lambda_2/\lambda_1 = 2$ requirement. It should be noted, however, that it is necessary to use several different dyes in order to achieve this range of wavelengths. For a typical broadband laser dye such as Coumarin 6, the range is from 510 nm to 550 nm, which only gives us a λ_2/λ_1 of 1.08. For Ti:Sapphire lasers, the range is 690 nm to 1025 nm, which gives us a λ_2/λ_1 of 1.48.

As a specific example, consider the case where $N_p = 1000$, $n = 2.2$, and $\lambda_1 = 500$ nm. We plot N/A as a function of L (where N/A has been optimized with respect to δ) for various values of λ_2/λ_1. The result is shown in Figure 8. We see that N/A saturates for large L (around 5 cm) as expected, and the saturation value is largest for $\lambda_2/\lambda_1 = 2$. In Figure 9, we plot N/A and N_λ as functions of L for $\lambda_2/\lambda_1 = 1.08$ and

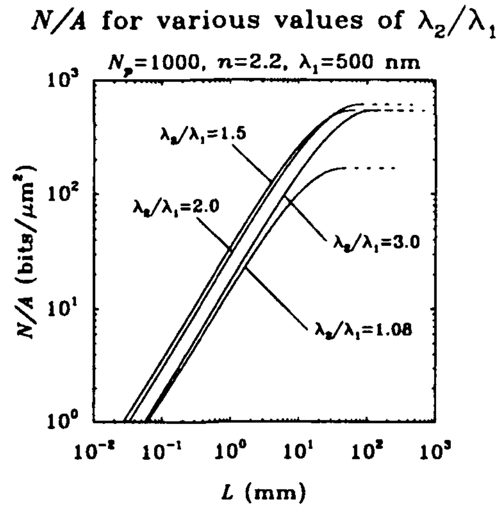

Figure 8. Wavelength multiplexing: optimum N/A (optimized with respect to δ) as a function of L for various values of λ_2/λ_1. We take $\lambda_1 = 500$ nm, $N_p = 1000$, and $n = 2.2$.

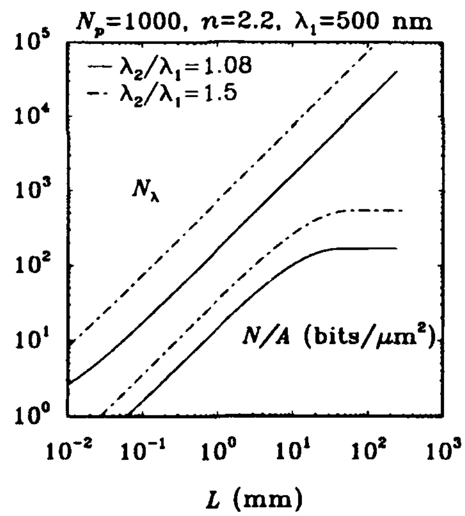

Figure 9. Wavelength multiplexing: optimum N/A and N_λ as functions of thickness L for $\lambda_2/\lambda_1 = 1.08$ and $\lambda_2/\lambda_1 = 1.5$. We take $\lambda_1 = 500$ nm, $N_p = 1000$, $n = 2.2$.

$\lambda_2/\lambda_1 = 1.5$ using the same N_p, n, and λ_1. For $\lambda_2/\lambda_1 = 1.08$, N/A approaches 166.0 bits/μm^2, while for $\lambda_2/\lambda_1 = 1.5$, N/A approaches 537.8 bits/μm^2.

3c. Storage Density and Optimum λ_2 for "Thin" Disks

The point where L causes N/A to reach saturation is of the order of 5 cm. At this thickness, it becomes questionable about what we mean by a "disk". In practice it may be desirable or necessary (e.g., because of

absorption) to keep the thickness small. In this case we are in the $L < L_{min}$ range (even though L_o may be larger than L_{min}), and N/A is given by Eq. (37). We can approximate Eq. (37) by

$$N/A \approx \frac{n}{2\delta_{min}^2}\left(\frac{1}{\lambda_1}-\frac{1}{\lambda_2}\right)L \propto \frac{1}{\lambda_2^2}\left(\frac{1}{\lambda_1}-\frac{1}{\lambda_2}\right), \tag{48}$$

if we assume that

$$\alpha x \gg 1 \gg \beta x. \tag{49}$$

In the previous example, $\alpha = 40$ for $\lambda_2/\lambda_1 = 1.08$, and $\alpha = 250$ $\lambda_2/\lambda_1 = 1.5$, while $\beta = 5.60 \times 10^{-3}$ in both cases, so the condition is satisfied.

If we limit x and hence the disk thickness L to the range required by Eq. (49), the optimum λ_2 can be found by taking the derivative of the expression in Eq. (48) with respect to λ_2 and setting it to zero. In this case, it is easy to show that the maximum N/A occurs for $\lambda_2/\lambda_1 = 1.5$ (again assuming that we are using the same λ_1), which is very close to the value provided by Ti:Sapphire lasers. Therefore, in this case the density does not increase indefinitely with $\Delta\lambda$.

Finally we can also calculate the "knee" of the N/A curve, which we define as the point were the expression given by Eq. (47) reaches the saturation value. This is given by

$$L = L_K = \frac{nN_p\delta_{min}^2}{4\lambda_2} = \frac{4z^2+1}{4}\,n\lambda_2 N_p, \tag{50}$$

which is proportional to λ_2. For $\lambda_2/\lambda_1 = 1.08$, $L_K = 11.0$ mm, which gives us $N/A = 106.5$ bits/μm^2 and $N_\lambda = 1,794$. For $\lambda_2/\lambda_1 = 1.5$, $L_K = 15.3$ mm, which gives us $N/A = 34.46$ bits/μm^2 and $N_\lambda = 11,221$. In both cases, L_K is less than L_{min}, and the corresponding values of N/A is slightly over half of the saturation values for N/A (i.e., approximately a 3 dB drop).

4. Discussion And Conclusions

The values for the various parameters discussed in this report are summarized in Table I, and the storage densities N/A are plotted in Figure 10 where we denote the densities of angle multiplexing and wavelength multiplexing by $(N/A)_\theta$ and $(N/A)_\lambda$, respectively.

In Figure 10, the curves for $(N/A)_\theta$ using just the angle range θ_1 to θ_2 (either as transmission or reflection holograms) is marked as ($\times$1). We see that it is about a factor of 2 smaller than $(N/A)_\lambda$. However, if we angle-multiplex from both sides of the signal beam, $(N/A)_\theta$ increases by a factor of 2 (denoted by the $\times$2 curve in Figure 10). If we further record both reflection and transmission holograms (as in Figure 3), this increases by a factor of 4 (denoted by the $\times$4 curve in Figure 10). In this case, $(N/A)_\theta$ becomes larger than $(N/A)_\lambda$ until L reaches about 12.5 mm, where both $(N/A)_\lambda$ and $(N/A)_\theta$ are about 115 bits/μm^2.

TABLE I. Value of Parameters used in Figure 10

(F/number of imaging lens is 3)

Parameters	**Angle multiplexing**	**Wavelength multiplexing**
Index of Refraction	$n = 2.2$	$n = 2.2$
Number of Pixels	$N_p^2 = 10^6$	$N_p^2 = 10^6$
Wavelength	$\lambda = 500$ nm	$\lambda_1 = 500$ nm, $\lambda_2 = 540$ nm
Angles	$\theta_1 = 10°$, $\theta_1 = 20°$,	—
Pixel Size	$\delta_{min} = 3.04\ \mu$m	$\delta_{min} = 3.28\ \mu$m
Critical Thickness	$L_{min} = 40.36$ mm	$L_{min} = 43.59$ mm
Optimum Thickness	$L_o = 16.74$ mm	$L_o \approx 30$ mm
Maximum Density	$N/A = 4 \times 29.3$ bits/μm^2	$N/A = 166.0$ bits/μm^2
Number of Holograms	$N_\theta = 1306$	$N_\lambda \approx 5000$

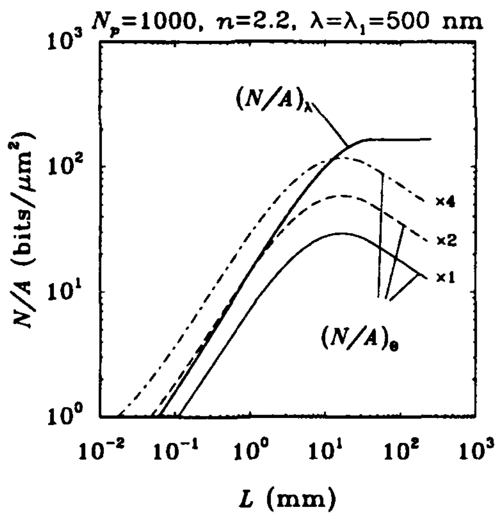

Figure 10. Comparison of angle multiplexing and wavelength multiplexing. We take $\lambda = \lambda_1 =$ 500 nm, $\lambda_2/\lambda_1 = 1.08$, $n = 2.2$, $N_p = 1000$, $\theta_1 = 10°$, and $\theta_2 = 20°$. The density using angle multiplexing is denoted by $(N/A)_\theta$, and the density using wavelength multiplexing is denoted by $(N/A)_\lambda$.

One might ask whether it is possible to achieve higher density by recording in the Fourier plane instead of the image plane. It turns out that the storage density is the same. This is because the space-bandwidth-product is a constant. Specifically, consider an image of extent $a = N_p\delta$, where δ is the pixel spacing and N_p is the number of pixels along one dimension. Let b be the extent of the Fourier transform of this image

(by a lens of focal length F), and let $1/\delta'$ be the highest spatial frequency of the Fourier transform. Then within the paraxial approximations

$$N_p = \frac{a}{\delta} = \frac{b}{\delta'}. \tag{51}$$

This shows that recording in either the image plane or the Fourier plane will give the same minimum width.

If we record holograms at off-image or off-Fourier planes, the required width w increases. However, it is sometimes desirable to do this for purpose of noise, image quality, and alignment sensitivity. The tradeoff between these requirements and storage density will have to be considered in the design of a practical system.

We have derived the optimum conditions for achieving the maximum storage density of a 3-D HD disk using either angle multiplexing or wavelength multiplexing. Such optimally designed disks can store information with area densities more than 100 bits/μm^2 with disk thickness approximately 1 mm. However, the limits to storage density derived in this report are only due to the geometry of the system. The storage density can also be limited by noise (cross-talk, detector noise, media defects, etc.) and the limited dynamic range of the recording medium. These limits to N/A (addressed in a separate report [13]) prove less restrictive than the geometric limits derived here. This is supported by recent experiments [14] where 1000 holograms were superimposed and reconstructed with extremely low probability of error in a lithium niobate crystal with 1 cm thickness. The parameters of this experiment were reasonably close to the optimum parameters we derived.

REFERENCES

[1] P.J. Van Heerden, "Theory of Optical Information Storage in Solids," *Appl. Optics*, **2**, 393–400 (1963).

[2] K. Bløtekjaer, "Limitations on Holographic Storage Capacity of Photochromic and Photorefractive Media," *Appl. Opt.* **18**, 57–67 (1979).

[3] D. von der Linde and A.M. Glass, "Photorefractive Effects for Reversible Holographic Storage of Information," *Appl. Phys.*, **8**, 85–100 (1975).

[4] J.-P. Huignard, J.-P. Herriau, and F.. Micheron, "Coherent Selective Erasure of Superimposed Volume Holograms in $LiNbO_3$," *Appl. Phys. Lett.*, **26**, 256–258 (1975).

[5] L. d'Auria, J.-P. Huignard, C. Slezak, and E. Spitz, "Experimental Holographic Read-Write Memory using 3-D Storage," *Appl. Opt.*, *13*, 808–818 (1974).

[6] Y. Nakagome, H. Tanaka, K. Takeuchi, E. Kume, Y. Watanabe, T. Kaga, Y. Kawamoto, F. Murai, R. Izawa, D. Hisamoto, T. Kisu, T. Nishida, E. Takeda, and K. Itoh, "An Experimental 1.5-V 64-Mb DRAM," *IEEE J. Solid State Circuits*, **26**(4), 465–472 (1991).

[7] D. Psaltis,"Parallel optical memories", *Byte*, **17**(9), 179–182 (1992).

[8] H. Kogelnik, "Coupled Wave Theory for Thick Hologram Gratings," *Bell Syst. Tech. J.*, **48(9)**, 2909–2947 (1969).

[9] C. Gu, J. Hong, I. McMichael, Ragini Saxena, and F.H. Mok, "Cross Talk Limited Storage Capacity of Volume Holographic Memory," *J. OSA. A*, **9**, 1–6 (1992).

[10] F.H. Mok, "Applications of Holographic Storage in Lithium Niobate," (presented at OSA 1992 Annual Meeting) *OSA 1992 Annual Meeting Technical Digest*, Vol. 23, **WE1**, 102, Sept 1992.

[11] F.T.S. Yu, S.D. Wu, A.W. Mayers, and S.M. Rajan, "Wavelength Multiplexed Reflection Matched Spatial Filters Using $LiNbO_3$," *Opt. Comm.*, **81**(6), 343–347 (1991).

[12] G.A. Rakuljic, V. Leyva, and A. Yariv, "Optical-data Storage by using Orthogonal Wavelength-Multiplexed Volume Holograms," *Opt. Lett.*, **17**(20), 1471–1473 (1992).

[13] H.-Y. Li and D. Psaltis, "3-D Holographic Disks: Material Considerations," to be published.

[14] F. Mok, D. Psaltis, and G. Burr, "Spatial and Angle Multiplexed Holographic Random Access Memory," SPIE vol. 1773c, San Diego, CA, July 1992.

FIGURE CAPTIONS

1. The 3-D holographic disk (HD).
2. Recording geometry.
3. Angular multiplexing by reflection and transmission holograms from both sides of the signal beam.
4. Angle multiplexing: extra area taken up by defocusing and reference beam angle change.
5. Angle multiplexing: N/A vs. L for various values of θ_2. We take $N_p = 1000$, $n = 2.2$, $\lambda = 500$ nm, and $\theta_1 = 10°$.
6. Angle multiplexing: optimum N/A (optimized with respect to δ) and N_p as functions of thickness L. We take $N_p = 1000$, $n = 2.2$, $\lambda = 500$ nm, $\theta_1 = 10°$, and $\theta_2 = 20°$.
7. Wavelength multiplexing: extra area taken up because of defocusing and wavelength change.
8. Wavelength multiplexing: optimum N/A (optimized with respect to δ) as a function of L for various values of λ_2/λ_1. We take $\lambda_1 = 500$ nm, $N_p = 1000$, and $n = 2.2$.
9. Wavelength multiplexing: optimum N/A and N_λ as functions of thickness L for $\lambda_2/\lambda_1 = 1.08$ and $\lambda_2/\lambda_1 = 1.5$. We take $\lambda_1 = 500$ nm, $N_p = 1000$, $n = 2.2$.
10. Comparison of angle multiplexing and wavelength multiplexing. We take $\lambda = \lambda_1 = 500$ nm, $\lambda_2/\lambda_1 = 1.08$, $n = 2.2$, $N_p = 1000$, $\theta_1 = 10°$, and $\theta_2 = 20°$. The density using angle multiplexing is denoted by $(N/A)_\theta$, and the density using wavelength multiplexing is denoted by $(N/A)_\lambda$.